Electronic Supplementary Material (ESI) for New Journal of Chemistry.

SUPPORTING INFORMATION

Influence of (de)protonation on the photophysical properties of phenol-substituted diazine chromophores: experimental and theoretical studies

Maxime Hodée,[a] Augustin Lenne,[a] Julian Rodríguez-López,[b] Françoise Robin-le Guen,[a] Claudine Katan,[a] Sylvain Achelle,[a*] and Arnaud Fihey.[a*]

[a] Univ Rennes, CNRS, ISCR (Institut des Sciences Chimiques de Rennes) - UMR 6226, F-35000 Rennes, France. E-mails: sylvain.achelle@univ-rennes1.fr, arnaud.fihey@univ-rennes1.fr

[b] Universidad de Castilla-La Mancha, Área de Química Orgánica, Facultad de Ciencias y Tecnologías Químicas, Avda. Camilo José Cela 10, 13071 Ciudad Real, Spain

Table S1. Computed free energy difference and corresponding Boltzmann population for the different configurations and conformations of compounds **1-7** and **3OMe** (see Figure 2 in the main text for their representation).

Compd		ΔG (kJ·mol^{-1})	%pop
1		/	100
2	*(Z)*	22.52	0
	(E)	0.00	100
3	A	0.00	84
	B	4.18	16
3OMe	A	0.00	83
	B	3.99	17
4	*(Z)*	21.75	0
	(E)	0.00	100
5	A	0.00	87
	B	4.63	13
6	A	0.00	88
	B	5.03	12
7	*(Z)*	14.16	0
	(E)	0.00	100

Table S2. Dihedral angle between the phenolic group and the aromatic ring of the linker computed for compounds **1-7** in their neutral (n) protonated (p), and deprotonated forms (wB97XD/6-311+G(d,)/DMSO). GS stands for the ground state geometry and ES for the excited state geometry.

	1		**2**		**3**		**3OMe**		**4**		**5**		**6**		**7**	
	GS	ES	GS	ES	GS	ES	GS	ES	GS	ES	GS	ES	GS	ES	GS	ES
n	39	3	39	18	32	0	32	0	31	0	32	0	31	0	39	19
p	38	5	38	17	-30	0	29	0	30	0	31	0	28	0	38	17
d	31	4	31	3	21	0	/	/	22	0	22	0	20	0	31	2

Table S3. Computed energy levels (in eV) of the frontier orbitals and electronic gaps for neutral compounds **1**-**7**.

	1	**2**	**3**	**3OMe**	**4**	**5**	**6**	**7**
HOMO	-8.05	-7.82	-7.82	-7.77	-7.55	-7.72	-7.71	-8.05
LUMO	-0.31	-0.69	-0.55	-0.55	-0.77	-0.46	-0.85	-0.90
Gap	7.74	7.13	7.27	7.22	6.77	7.26	6.86	7.15

Table S4. Computed energy levels (in eV) of the frontier orbitals and electronic gap for protonated compounds **1**-**7**.

	1	**2**	**3**	**3OMe**	**4**	**5**	**6**	**7**
HOMO	-8.23	-8.02	-8.10	-8.04	-7.79	-8.00	-8.15	-7.97
LUMO	-1.61	-1.76	-1.69	-1.69	-1.80	-1.69	-2.15	-1.63
Gap	6.62	6.27	6.41	6.35	5.98	6.30	6.00	6.34

Table S5. Computed energy levels (in eV) of the frontier orbitals and electronic gap for deprotonated compounds **1**-**7**.

	1	**2**	**3**	**4**	**5**	**6**	**7**
HOMO	-6.48	-6.44	-6.43	-6.35	-6.40	-6.41	-6.42
LUMO	-0.16	-0.57	-0.36	-0.64	-0.27	-0.71	-0.42
Gap	6.32	5.87	6.07	5.71	6.13	5.69	6.01

Table S6. Bond length alternation (BLA) values for compounds **1**-**7** in their neutral (**n**), protonated (**p**) and deprotonated (**d**) forms. The conjugation paths used to define the BLA are shown in Figure S1.

		1	**2**	**3**	**3OMe**	**4**	**5**	**6**	**7**
n	**GS**	0.0111	0.0073	0.0081	0.0080	0.0070	0.0097	0.0082	0.0074
	ES	0.0021	0.0010	0.0000	-0.0001	0.0012	0.0001	0.0000	0.0008
p	**GS**	0.0090	0.0051	0.0047	0.0036	0.0043	0.0069	0.0042	0.0049
	ES	0.0014	0,0000	-0.0004	-0.0007	0.0000	0.0021	0.0001	-0.0004
d	**GS**	0.0057	0.0031	0.0021	/	0.0025	-0.0039	0.0024	0.0033
	ES	-0.0035	-0.004	-0.0059	/	-0.0042	-0.0056	-0.0079	-0.0033

Table S7. Computed Mulliken atomic partial charges on the two nitrogen atoms for **1**-**7**.

Compd	N_1	N_3 / N_4
1	-0.183	-0.072
2	-0.190	-0.133
3	-0.188	-0.111
3OMe	-0.186	-0.111
4	-0.111	-0.840
5	-0.108	-0.530
6	-0.061	0.065
7	-0.109	-0.097

Table S8. Comparison of the computed optical properties for the two possible protonated forms of compound **3**.

Compd	λ_{abs} [nm] (*f*) E_{abs} [eV]	Orbital contributions	λ_{em} [nm] (*f*) E_{em} [eV]	Orbital contributions
3 (protonated on N_1)	382 (1.06) 3.25	HOMO → LUMO (86%)	504 (1.41) 2.46	HOMO → LUMO (94%)
3 (protonated on N_3)	378 (1.08) 3.28	HOMO → LUMO (86%)	503 (1.42) 2.46	HOMO → LUMO (94%)

On the choice of the computational method

Table S9 compares the impact of the nature of the XC functional and the solvent model on the computed absorption and emission energies of compounds **1**-**4**. Table S10 compares the E^{0-0} energies for **1-7** obtained with two different functionals. All calculations were conducted with a 6-311+G(d,p) basis set. From Table S9 it appears that the ωB97X-D functional provides the best agreement with the experimental emission, while the PBE0 functional reproduces better the experimental absorption. The experimental E^{0-0} energies are clearly more accurately reproduced with the ωB97X-D functional.

Overall, the SS-PCM model do not improve the description of the transition energies, and the LR-PCM/wB97X-D scheme appears to be the best suited to explore the excited state properties in this series of compounds. Thus, this method is retained as default computational protocol in all other sections.

Table S9. Comparison of the experimental and calculated values of the absorption/emission energies (in eV) within the Linear-Response (LR) and State Specific (SS) PCM (DMSO) formalism for neutral forms of **1-4** and **3OMe**, using two different functionals, PBE0 and ωB97X-D.

	LR-PCM PBE0	SS-PCM PBE0	LR-PCM ωB97X-D	SS-PCM ωB97X-D	Experimental
1	3.89 / 3.46	3.10 / 2.64	4.20 / 3.16	4.26 / 3.12	--
2	3.47 / 3.07	2.76 / 2.32	3.83 / 2.75	3.79 / 2.83	3.51 / 2.45
3	3.54 / 3.09	3.13 / 2.73	3.82 / 2.74	3.75 / 2.86	3.37 / 2.65
3OMe	3.49 / 3.06	3.07 / 2.68	3.80 / 2.72	3.72 / 2.83	3.40 / 2.74
4	3.13 / 2.28	2.78 / 2.43	3.60 / 2.36	3.42 / 2.57	3.11 / 2.34

Table S10. Comparison of the experimental E^{0-0} energies (in eV) with calculated values within the LR-PCM formalism for neutral forms of **1**-**7**.

	PBE0	ωB97X-D	exp
1	3.16	3.54	--
2	2.75	3.12	2.98
3	2.79	3.05	2.96
3OMe	2.76	3.03	3.03
4	2.42	2.70	2.70
5	2.76	3.04	2.96
6	2.52	2.88	2.69
7	2.78	3.15	3.02
MSE	0.34	0.06	--

Table S11. Experimental Absorption and emission maxima in toluene, CH_2Cl_2 and DMSO

	Toluene		**CH_2Cl_2**		**DMSO**	
	λ_{abs} (nm)	λ_{em} (nm)	λ_{abs} (nm)	λ_{em} (nm)	λ_{abs} (nm)	λ_{em} (nm)
2	335	421	335	439	353	506
3	358	424	358	432	368	467
3OMe	388	427	359	439	365	453
4	360	472	387	472	399	530
5	360	427	360	447	370	478
6	393	470	394	495	408	539
7	349	417	345	450	365	496

Charge transfer analysis

As defined by *Adamo et al.*,[1,2] the description of a charge transfer nature at the ES can be described with density-based indexes. First, the electronic densities of the ground and excited states are defined as $\rho_{GS}(r)$ and $\rho_{ES}(r)$. The electronic density change from the ground to the excited state is then written as:

$$\Delta\rho(r) = \rho_{ES}(r) - \rho_{GS}(r).$$

With this, we can define two functions collecting all points in space where we witness an augmentation ($\rho_+(r)$) or a diminution ($\rho_-(r)$) of the electronic density:

$$\rho_+(r) = \begin{cases} \Delta\rho(r) \; if \; \Delta\rho(r) > 0 \\ 0 \; if \; \Delta\rho(r) < 0 \end{cases} \qquad \rho_-(r) = \begin{cases} \Delta\rho(r) \; if \; \Delta\rho(r) < 0 \\ 0 \; if \; \Delta\rho(r) > 0 \end{cases}$$

[1] T. Le Bahers, C. Adamo and I. Ciofini, *J. Chem. Theory Comput.* 2011, **7**, 2498–2506.
[2] C. Adamo, T. Le Bahers, M. Savarese, L. Wilbraham, G. García, R. Fukuda, M. Ehara, N. Rega and I. Ciofini, *Coord. Chem. Rev.* 2015, **304–305**, 166–178.

$$\int \rho_-(r)\, dr = -\int \rho_+(r)\, dr$$

As such, we define the barycenters of the spatial regions associated with $\rho_+(r)$ and $\rho_-(r)$ as R_+ and R_-:

$$R_+ = \frac{\int r\rho_+(r)\, dr}{\int \rho_+(r)\, dr} = (x_+, y_+, z_+) \qquad R_- = \frac{\int r\rho_-(r)\, dr}{\int \rho_-(r)\, dr} = (x_-, y_-, z_-)$$

The distance between these two barycenters is the so-called charge transfer distance D_{CT}:

$$D_{CT} = |R_+ - R_-|$$

In the same philosophy, we can define the difference of partial atomic charges computed at excited state and ground state as $\delta q_i = q_i^{ES} - q_i^{GS}$ and as such we define two collections of atoms respectively q_i^+ and q_i^-.

$$q_i^+ = \begin{cases} \delta q_i \; if \; \delta q_i > 0 \\ 0 \; if \; \delta q_i < 0 \end{cases} \qquad q_i^- = \begin{cases} \delta q_i \; if \; \delta q_i < 0 \\ 0 \; if \; \delta q_i > 0 \end{cases}$$

And thus, the quantity of charge transferred upon the excitation, Q_{CT} is defined as:

$$Q_{CT} = \sum q_i^+ \equiv -\sum q_i^-$$

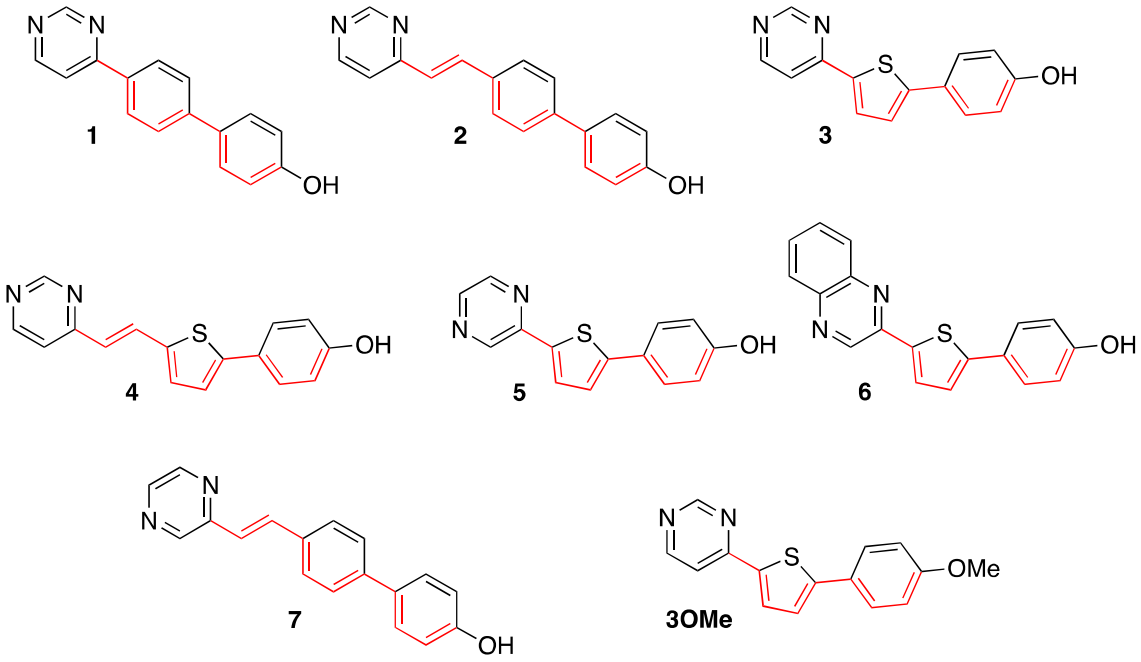

Figure S1. π-Conjugated pathway used in the bond length alternation value calculations.

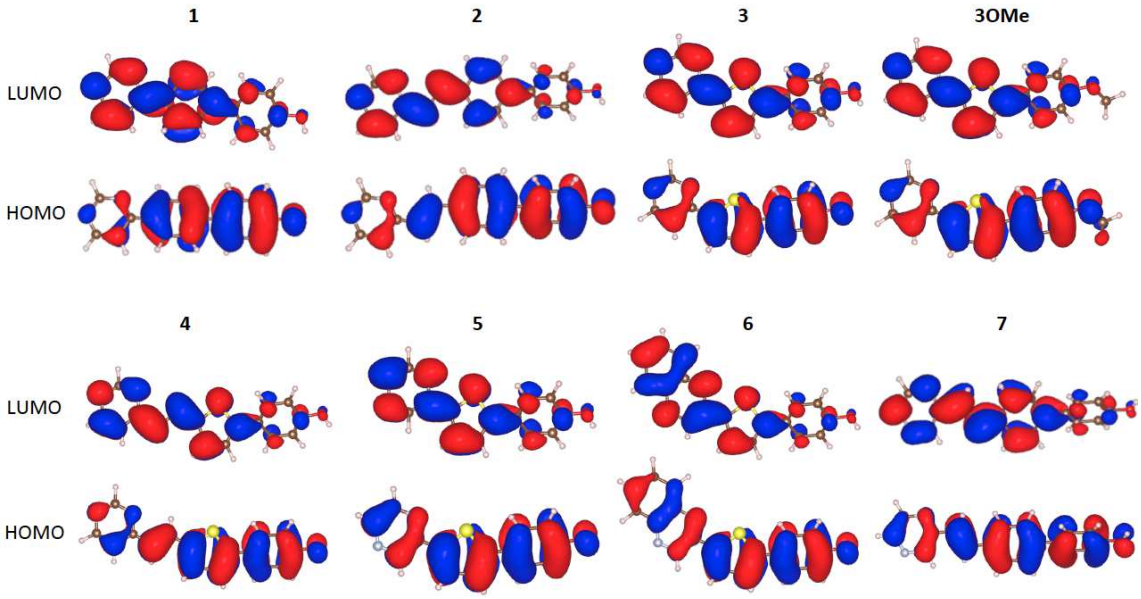

Figure S2. Frontier molecular orbitals for neutral compounds **1-7**.

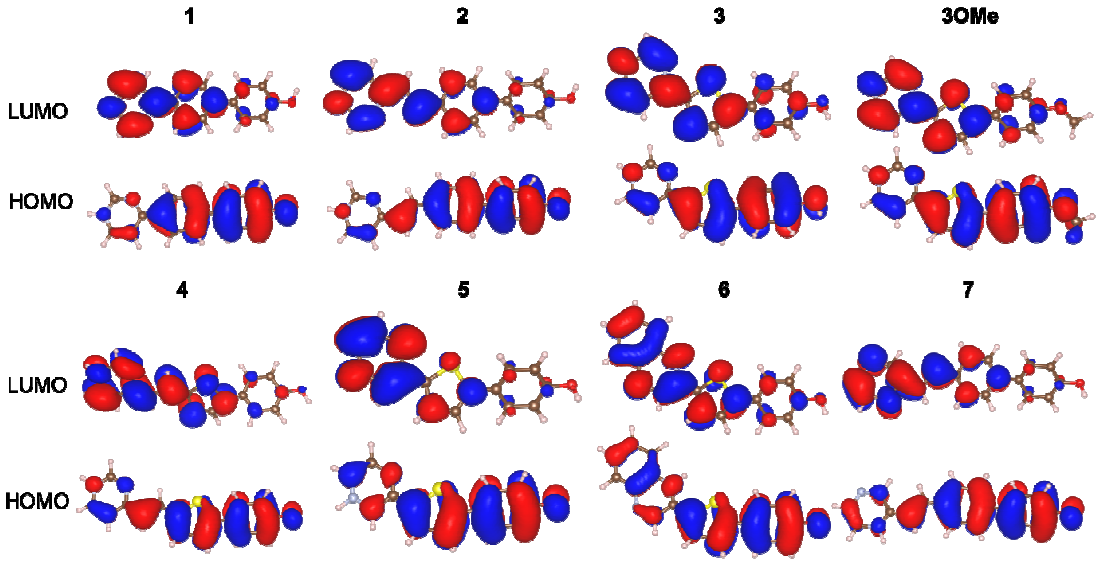

Figure S3. Frontier molecular orbitals for protonated compounds **1**-**7**.

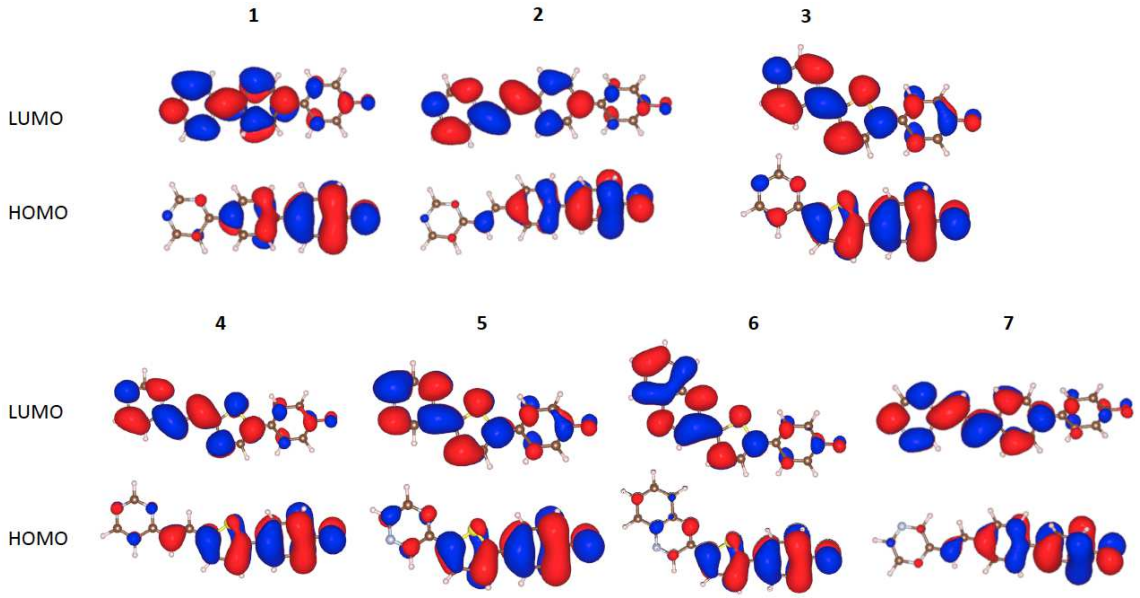

Figure S4. Frontier molecular orbitals for deprotonated compounds **1**-**7**.

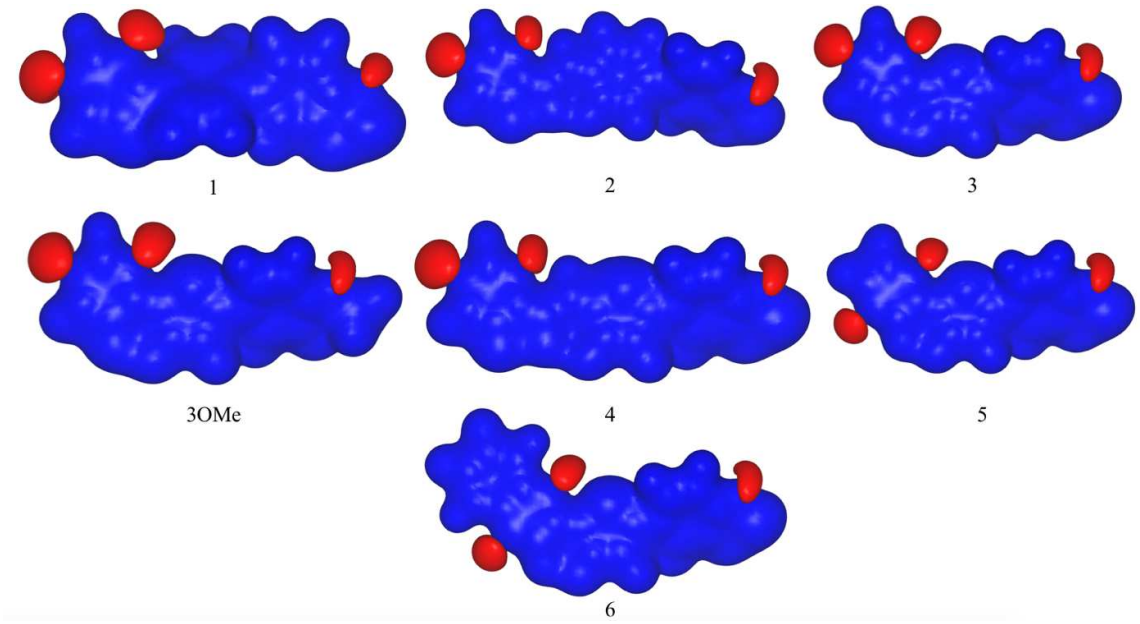

Figure S5. Electrostatic potential isosurfaces for neutral compounds **1**-**7**.

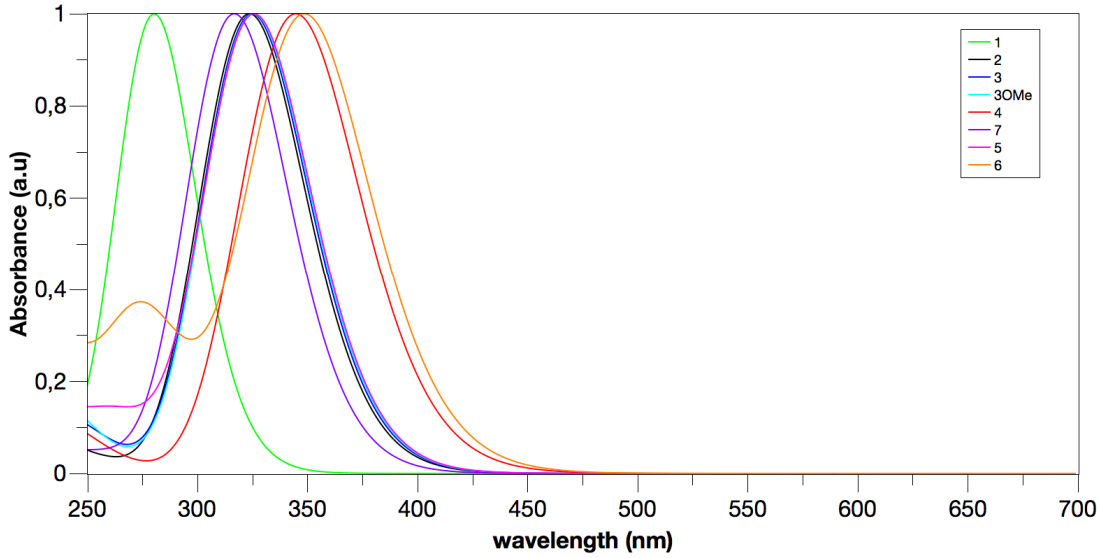

Figure S6. Computed absorption spectra for neutral compounds **1-7** in DMSO (FWHM: 0.3 eV).

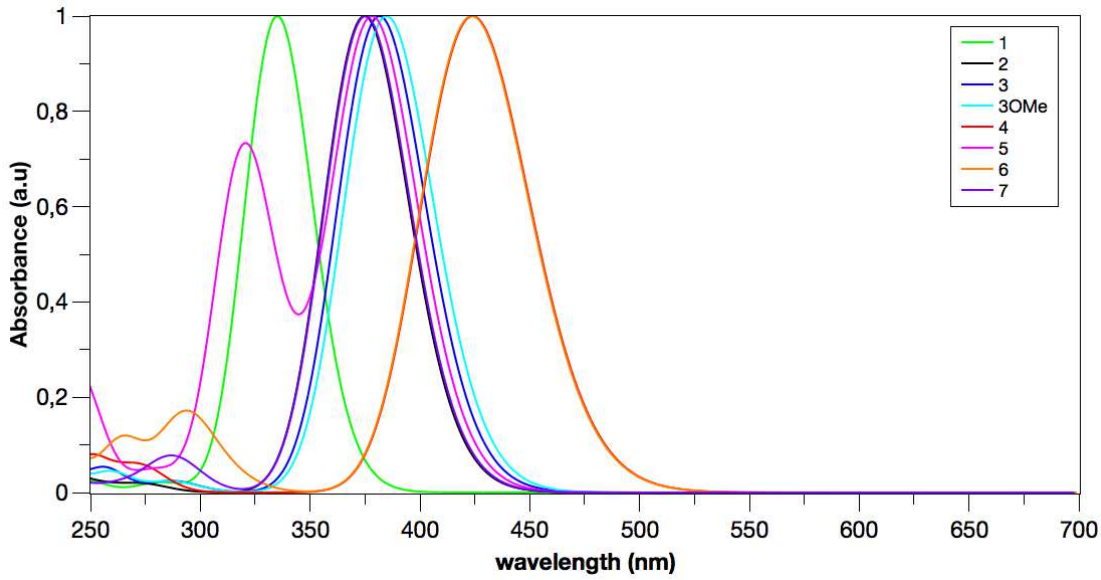

Figure S7. Computed absorption spectra for protonated compounds **1-7** in DMSO (FWHM: 0.3 eV).

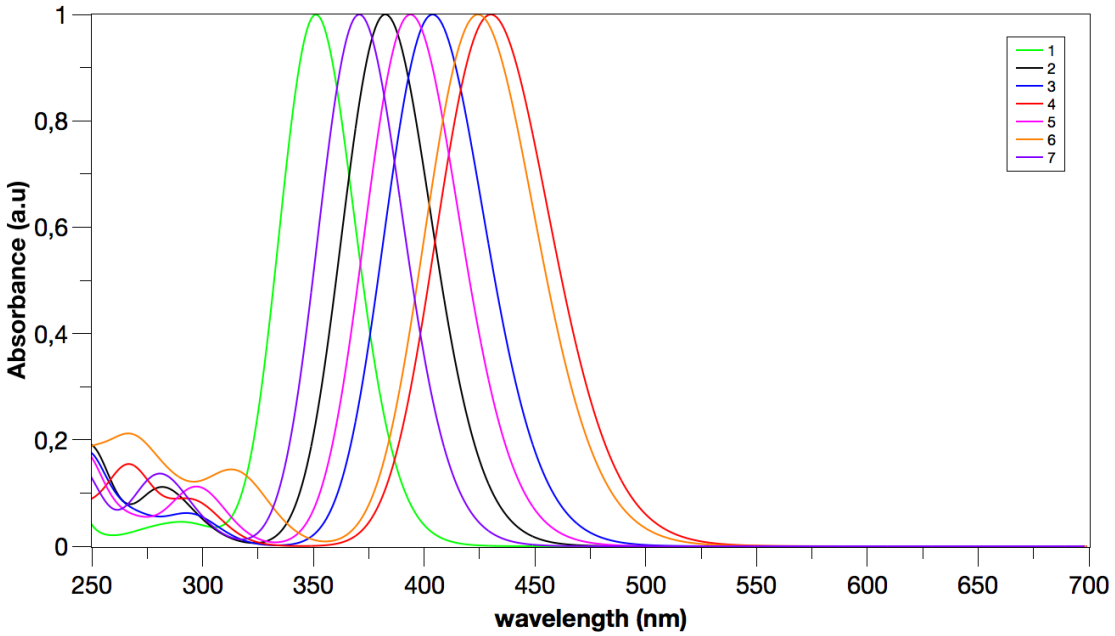

Figure S8. Computed absorption spectra for deprotonated compounds **1**-**7** in DMSO (FWHM: 0.3 eV).

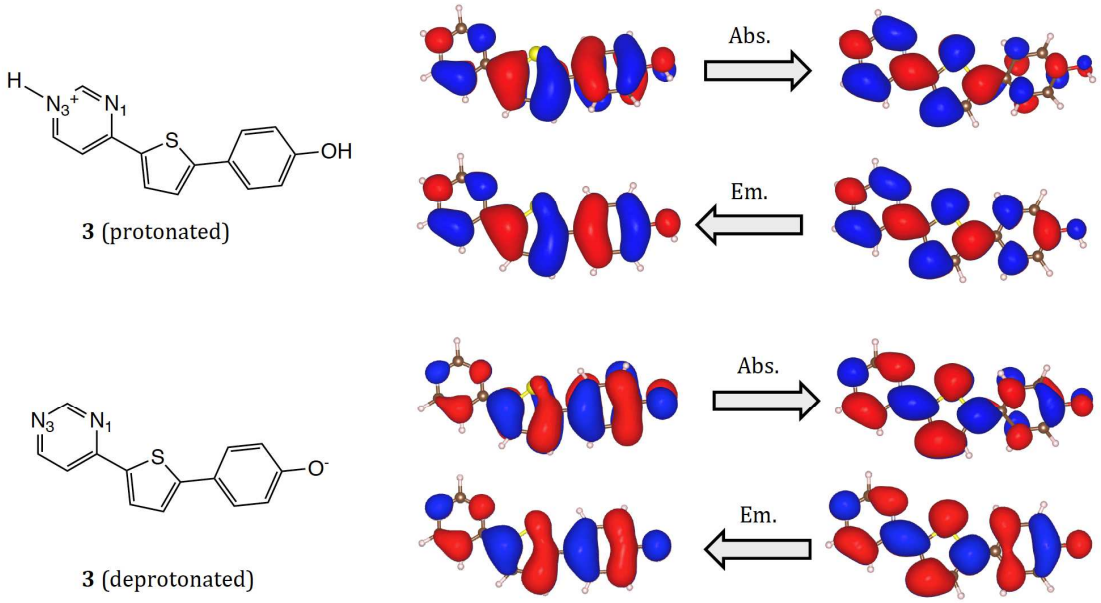

Figure S9. Natural transition orbitals (NTOs) for the first excited state of compound **3** in its protonated and deprotonated forms.

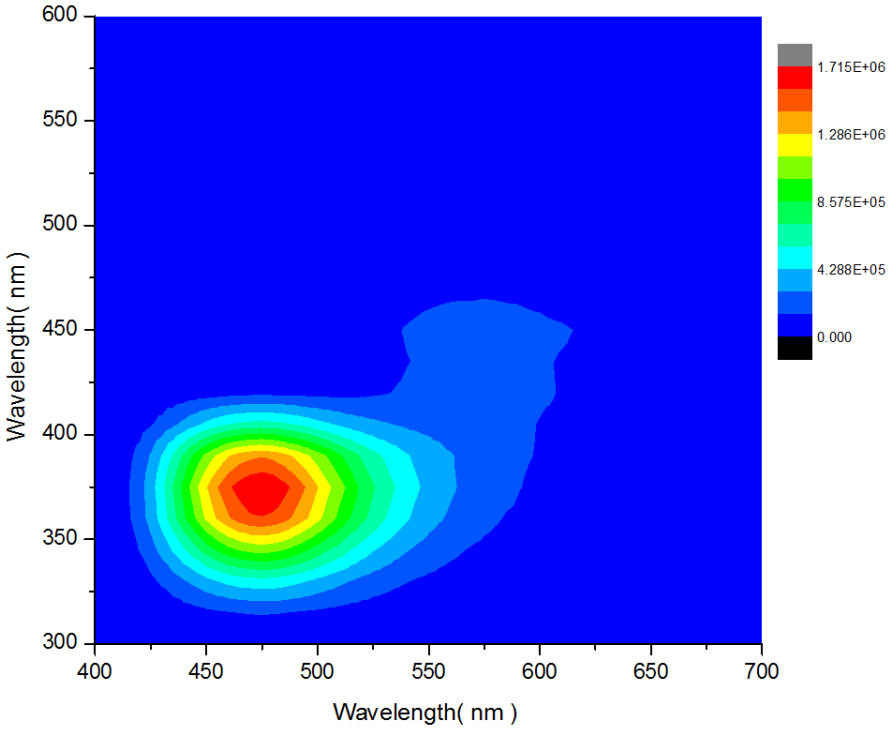

Figure S10. 2D fluorescence map for **3** in a 5 $\times 10^{-2}$ M solution of CSA in DMSO.

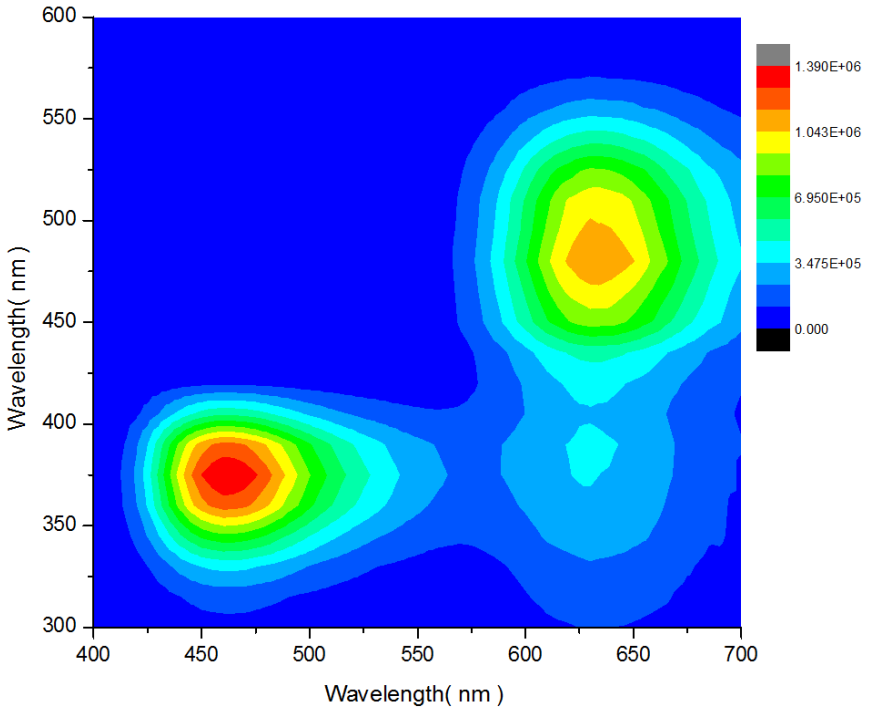

Figure S11. 2D fluorescence map for **3** in a 10^{-1} M solution of DBU in DMSO.

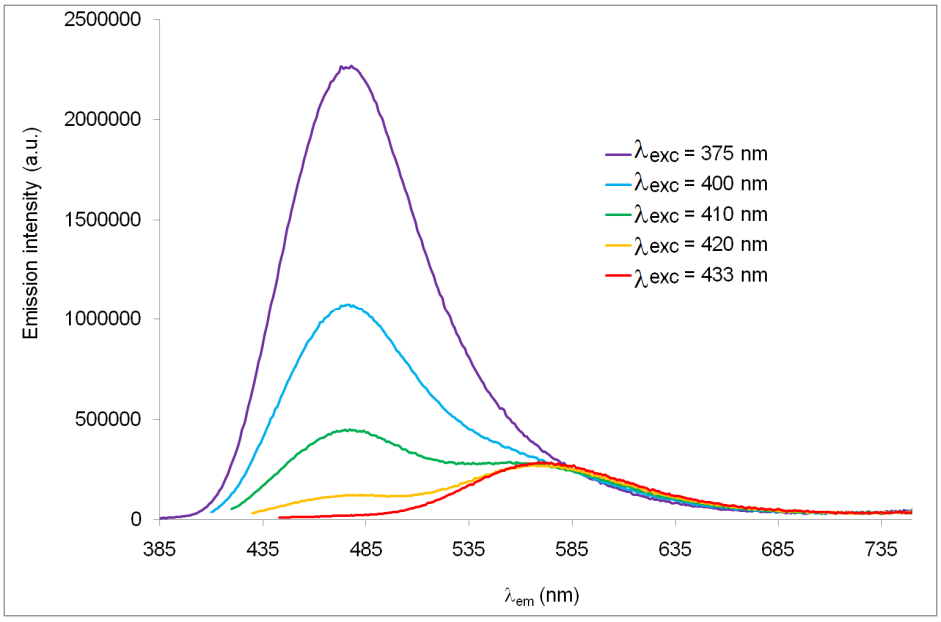

Figure S12. Changes in the emission spectra of **3** ($c = 1.75 \times 10^{-5}$ M) in a 10^{-1} M solution of CSA in DMSO as a function of the excitation wavelength.

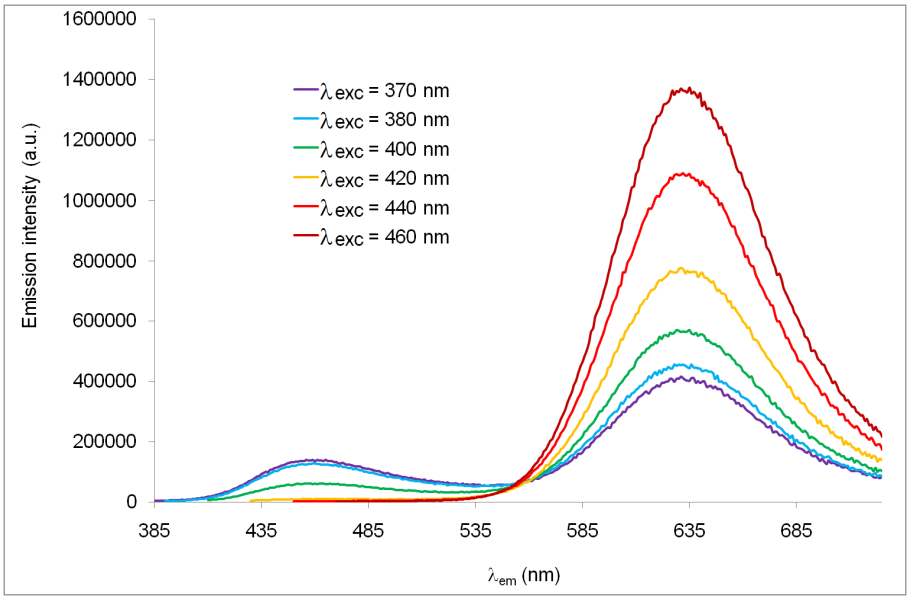

Figure S13. Changes in the emission spectra of **3** ($c = 1.75 \times 10^{-5}$ M) in a 10^{-1} M solution of DBU in DMSO as a function of the excitation wavelength.

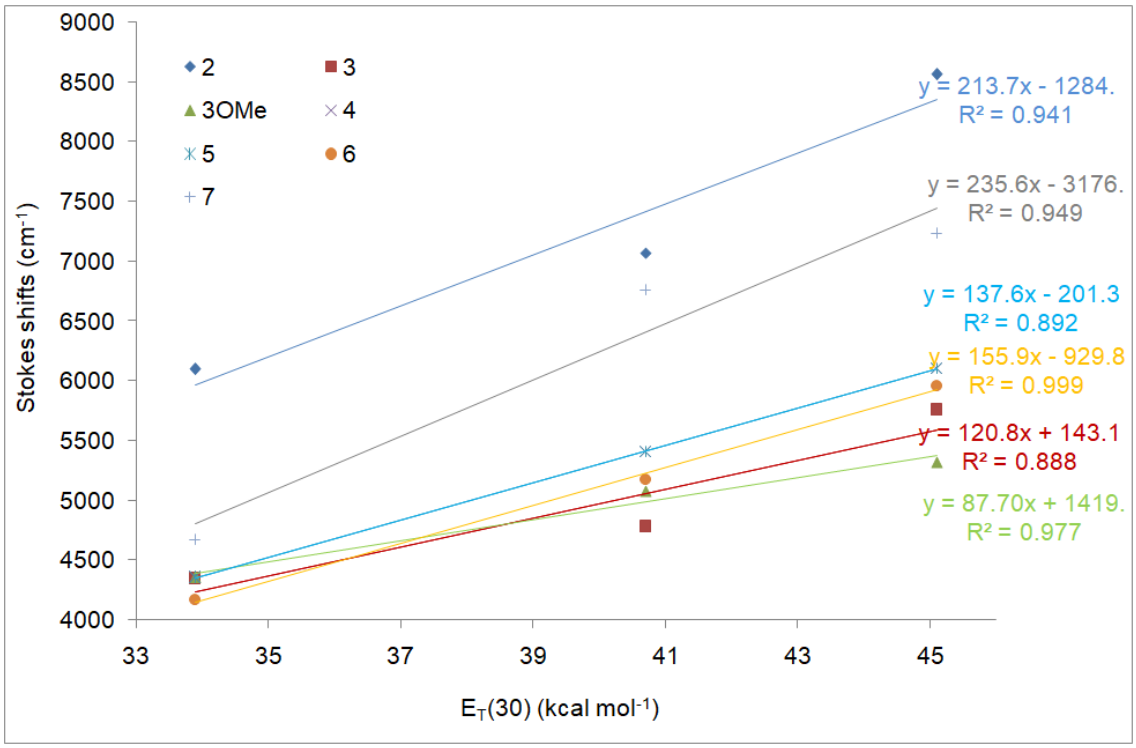

Figure S14: Plot of Stokes shifts versus Reichardt polarity pamameter ($E_T(30)$) for compound **2**-**7** and **3OMe** with data in Toluene, CH_2Cl_2 and DMSO

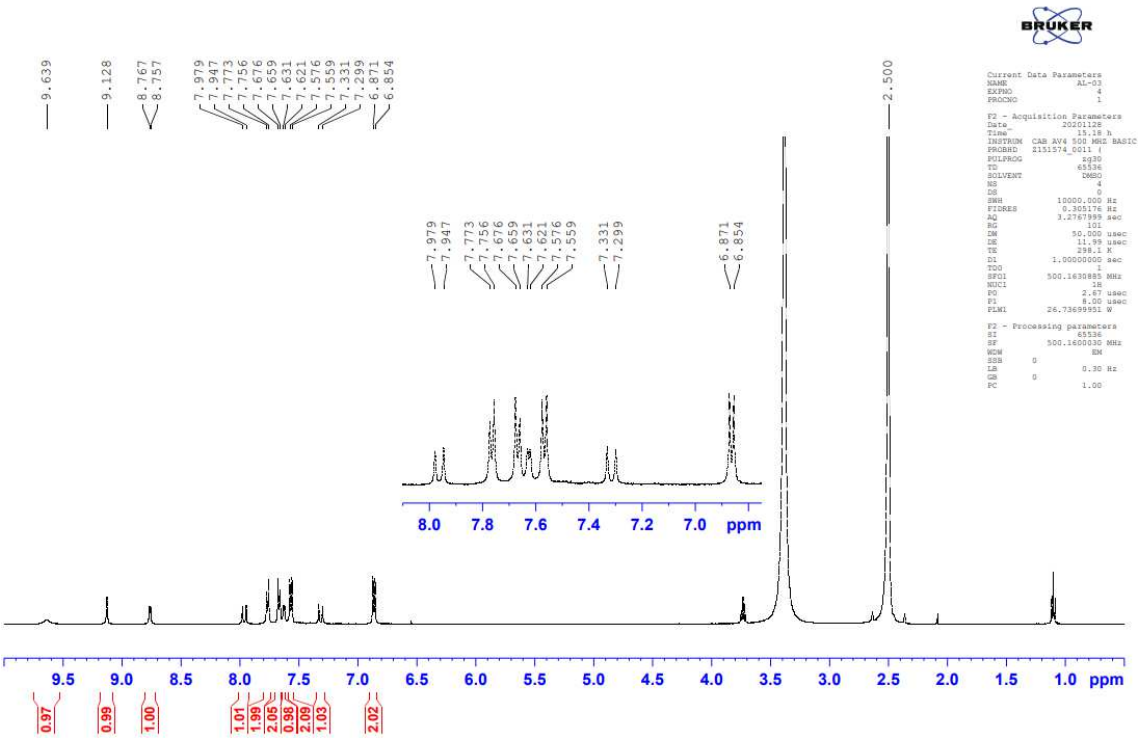

Figure S15. ^{1}H NMR spectrum of compound **2** (500 MHz, DMSO-d_6).

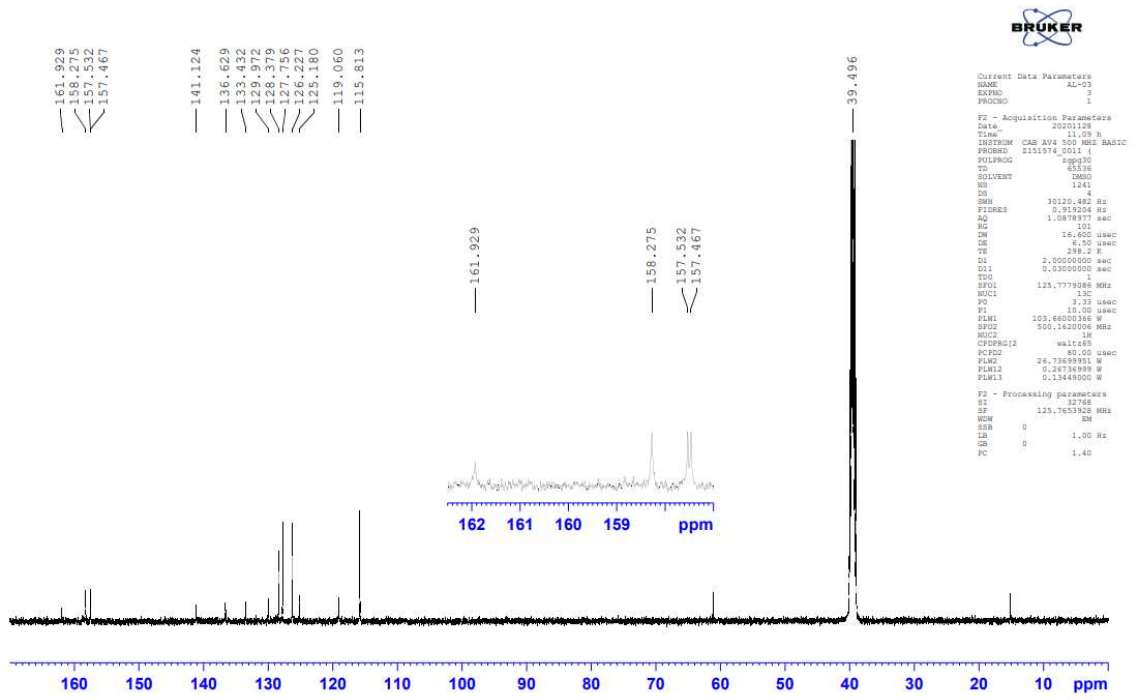

Figure S16. ^{13}C NMR spectrum of compound **2** (125 MHz, DMSO-d_6).

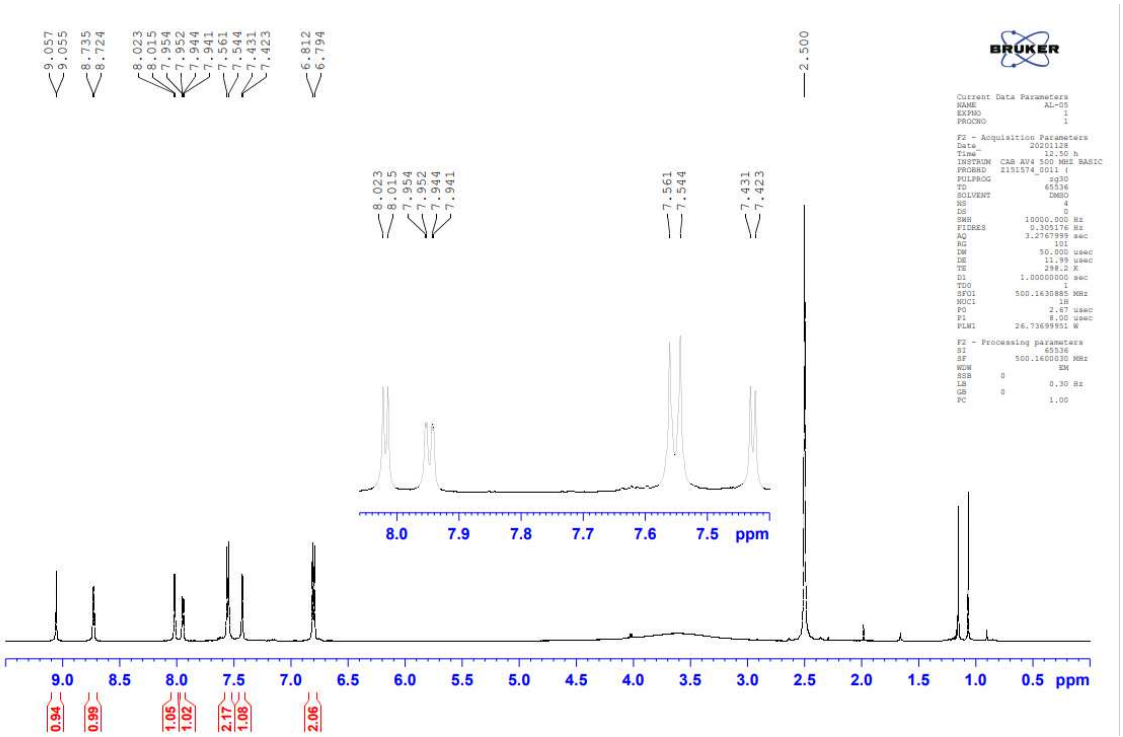

Figure S17. ^{1}H NMR spectrum of compound **3** (500 MHz, DMSO-d_6).

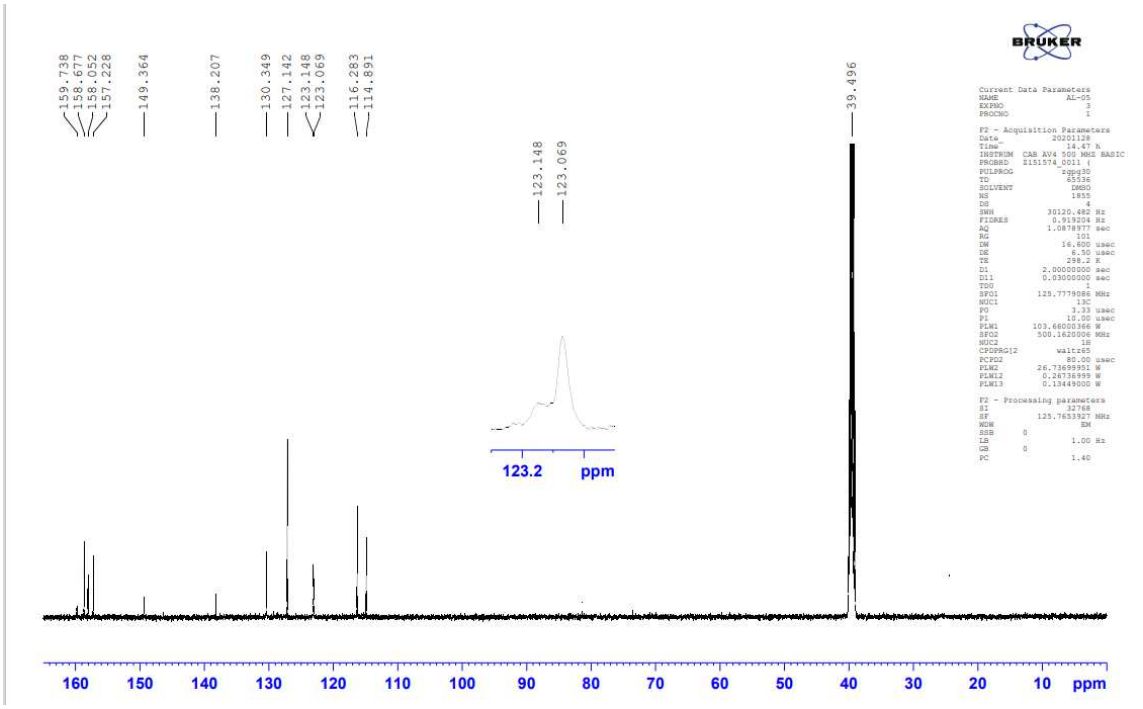

Figure S18. ^{13}C NMR spectrum of compound **3** (125 MHz, DMSO-d_6).

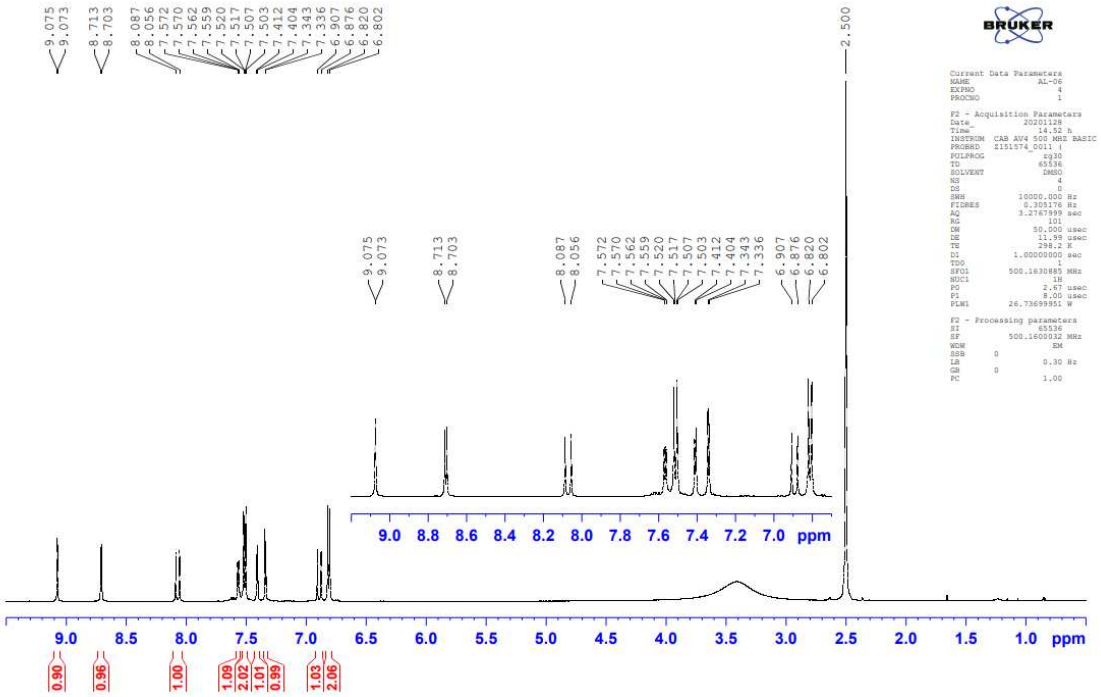

Figure S19. ^{1}H NMR spectrum of compound **4** (500 MHz, DMSO-d_6).

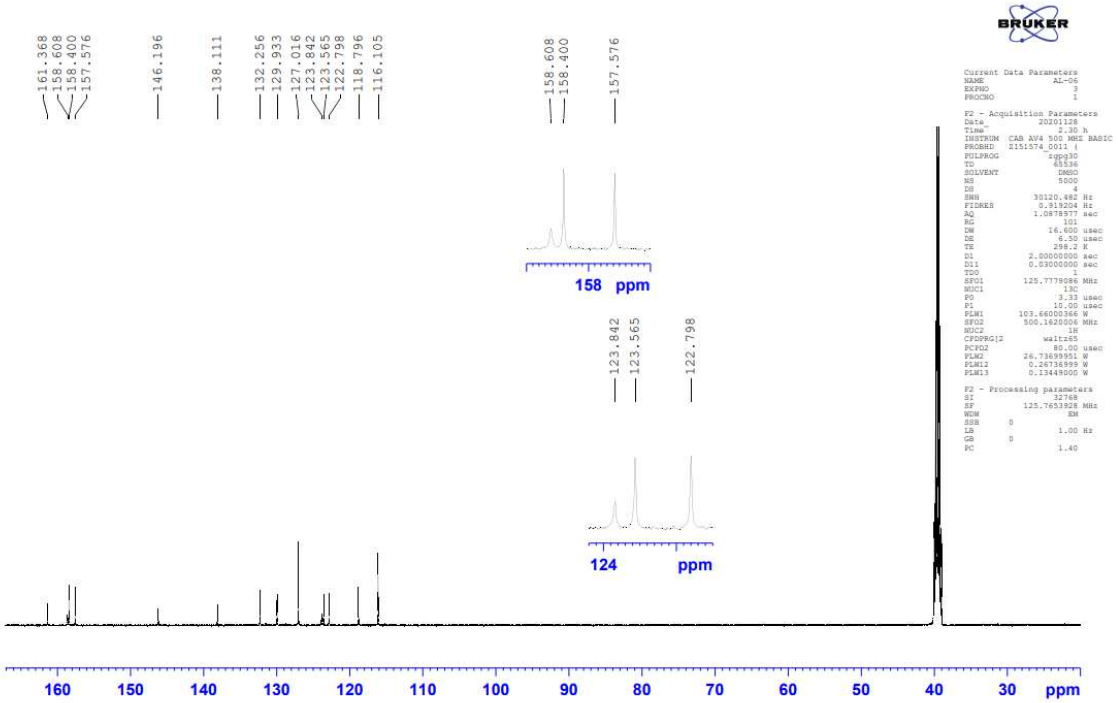

Figure S20. ^{13}C NMR spectrum of compound **4** (125 MHz, DMSO-d_6).

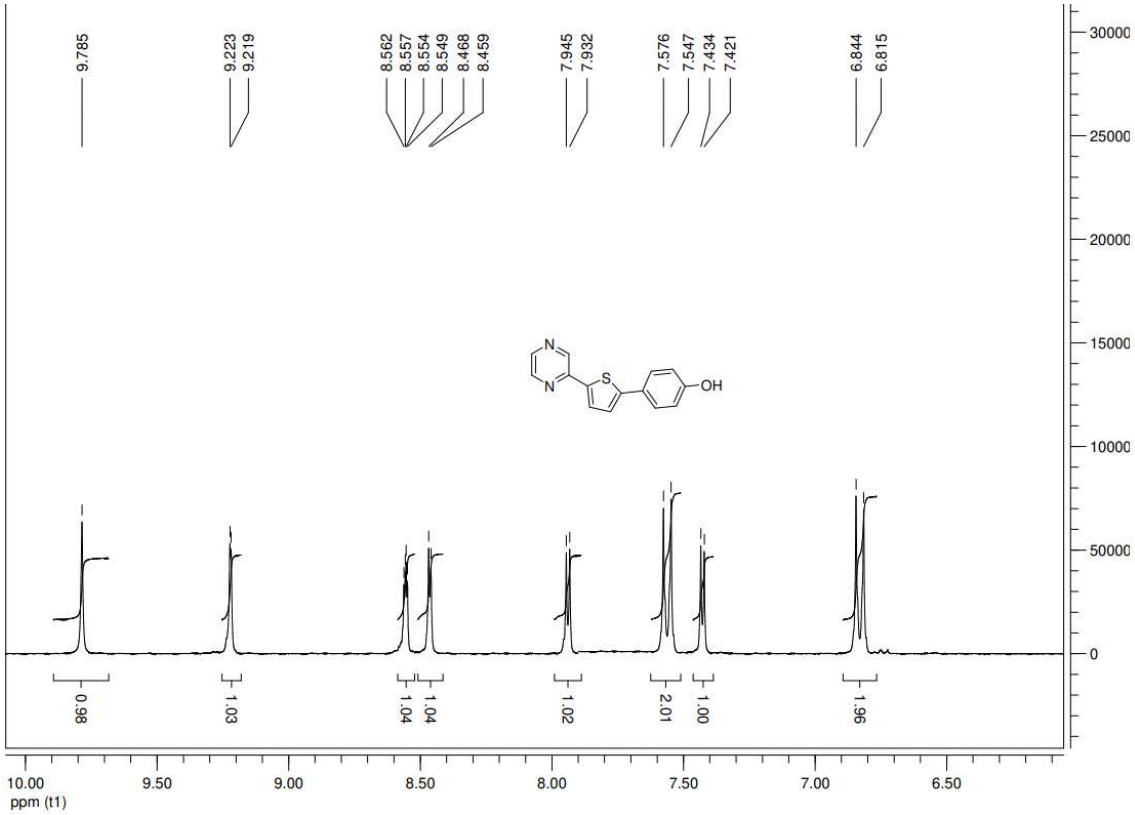

Figure S21. ^{1}H NMR spectrum of compound **5** (300 MHz, DMSO-d_6).

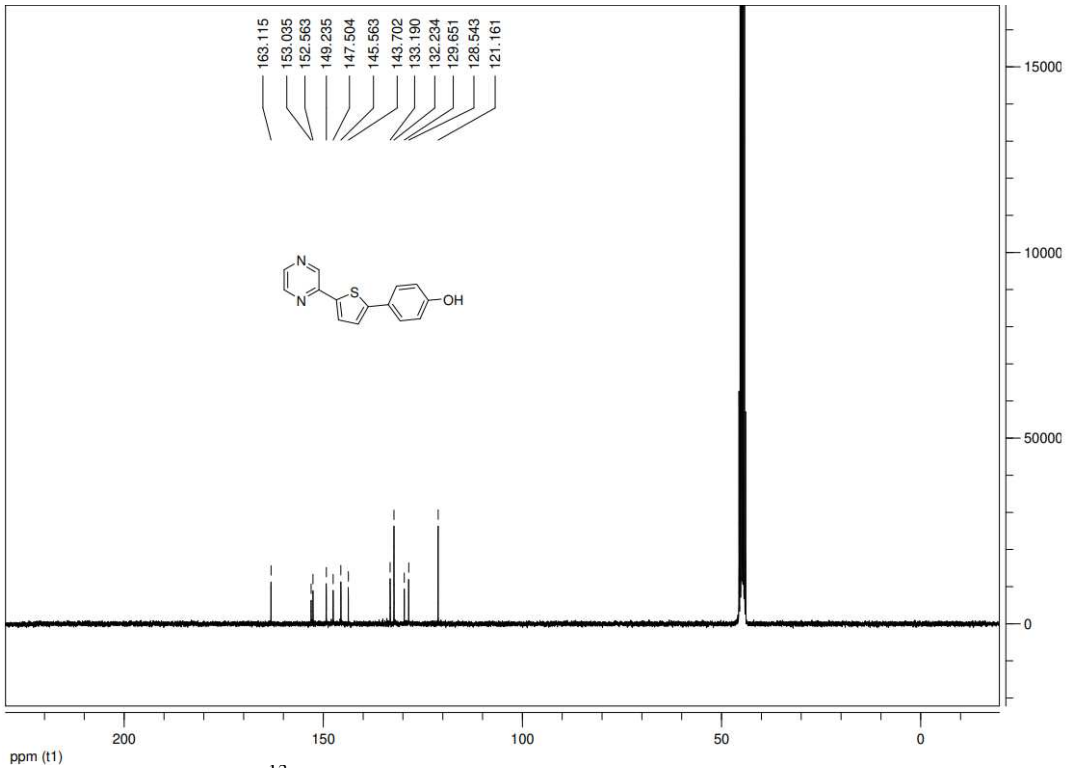

Figure S22. ^{13}C NMR spectrum of compound **5** (75 MHz, DMSO-d_6).

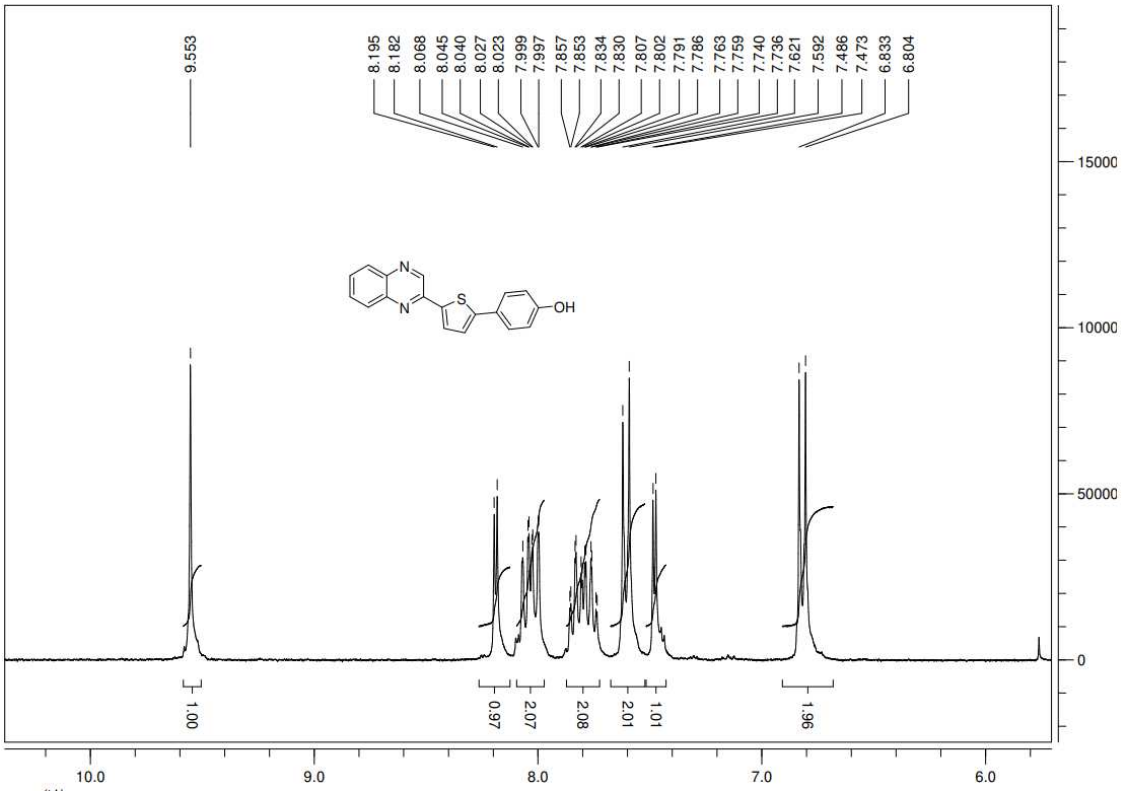

Figure S23. ^{1}H NMR spectrum of compound **6** (300 MHz, DMSO-d_6).

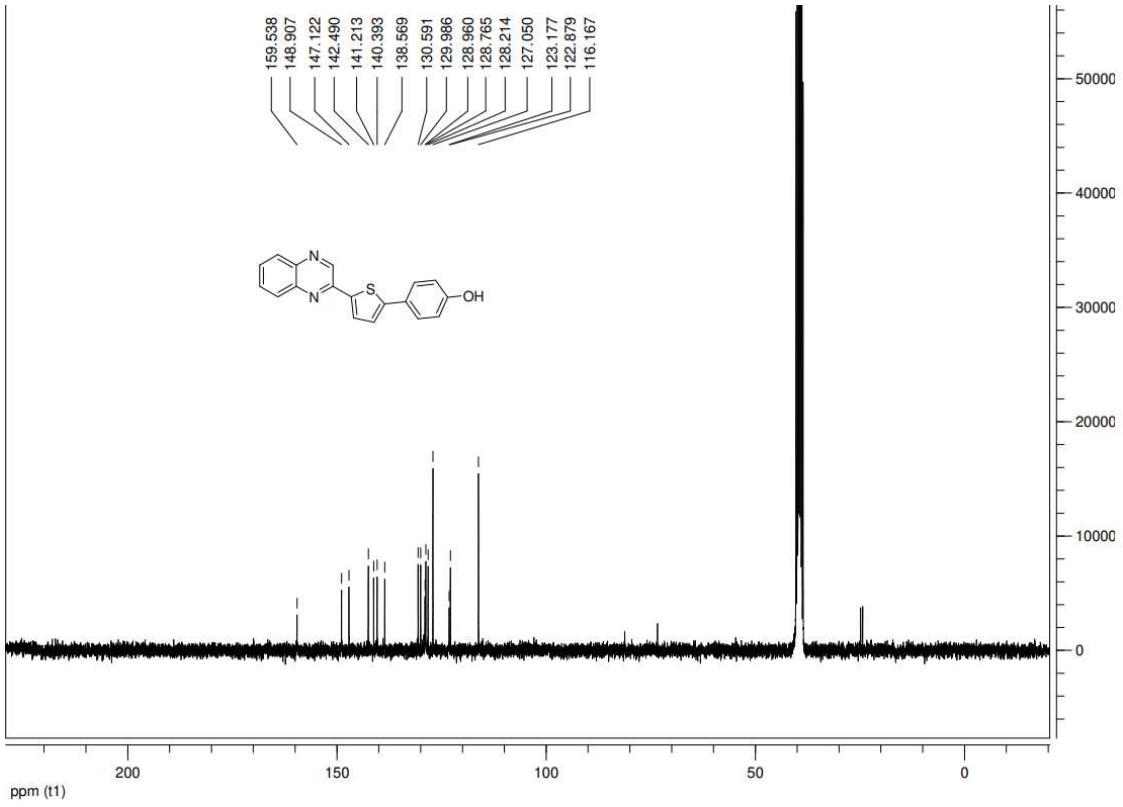

Figure S24. ^{13}C NMR spectrum of compound **6** (75 MHz, DMSO-d_6).

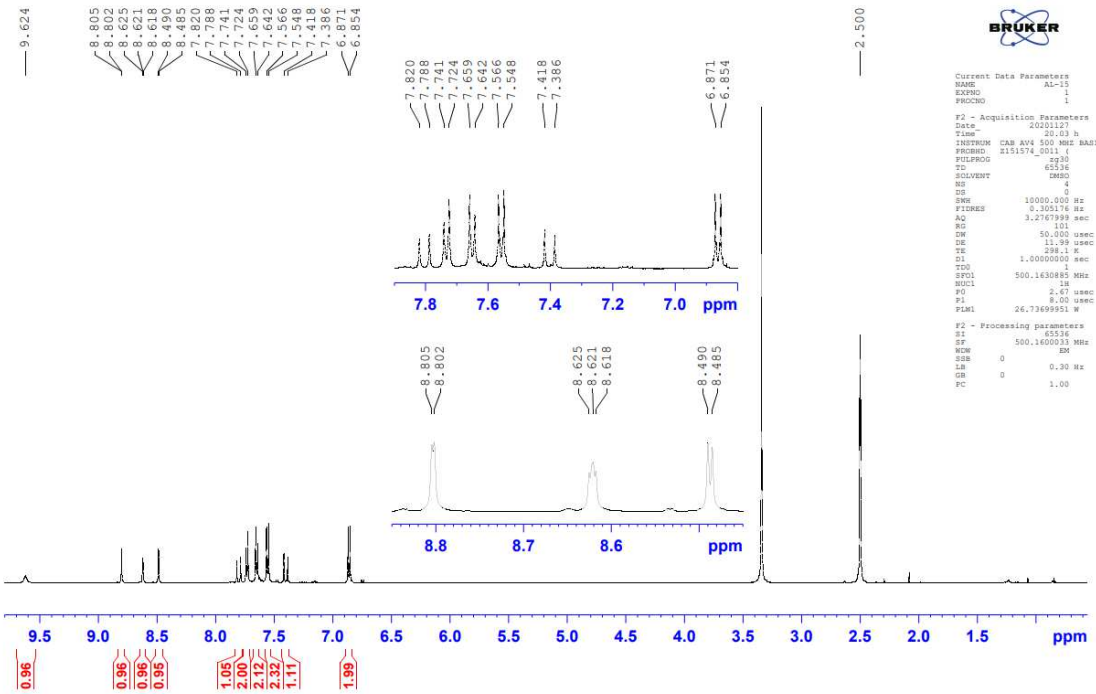

Figure S25. ^{1}H NMR spectrum of compound **7** (500 MHz, DMSO-d_6).

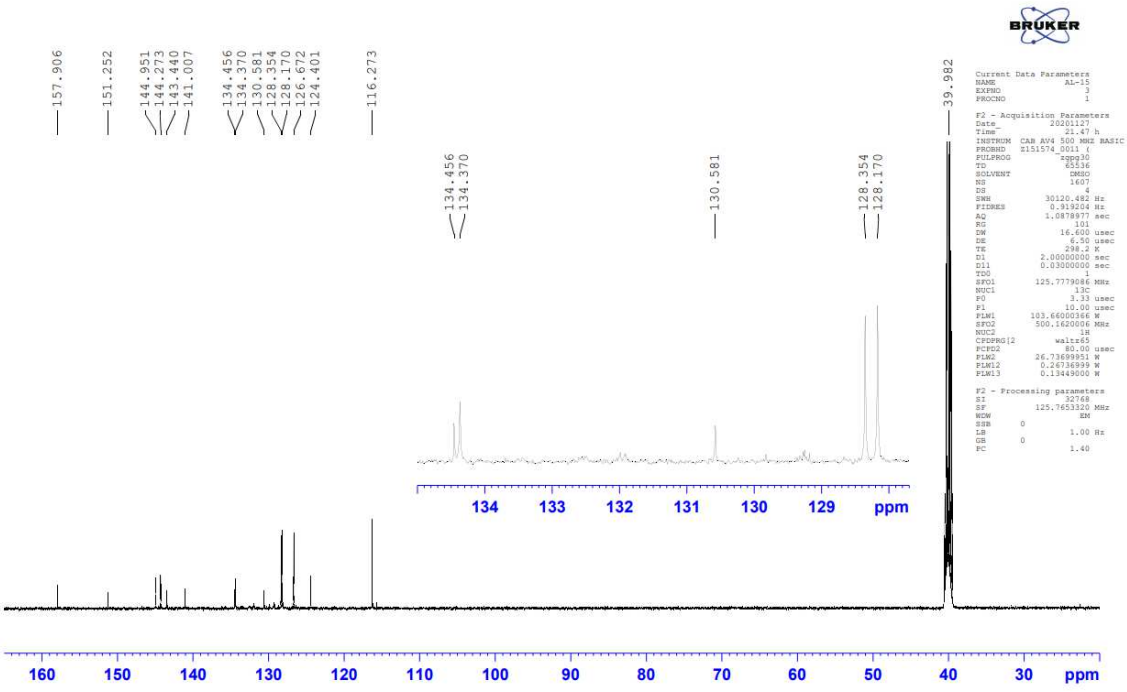

Figure S26. ^{13}C NMR spectrum of compound **7** (125 MHz, DMSO-d_6).

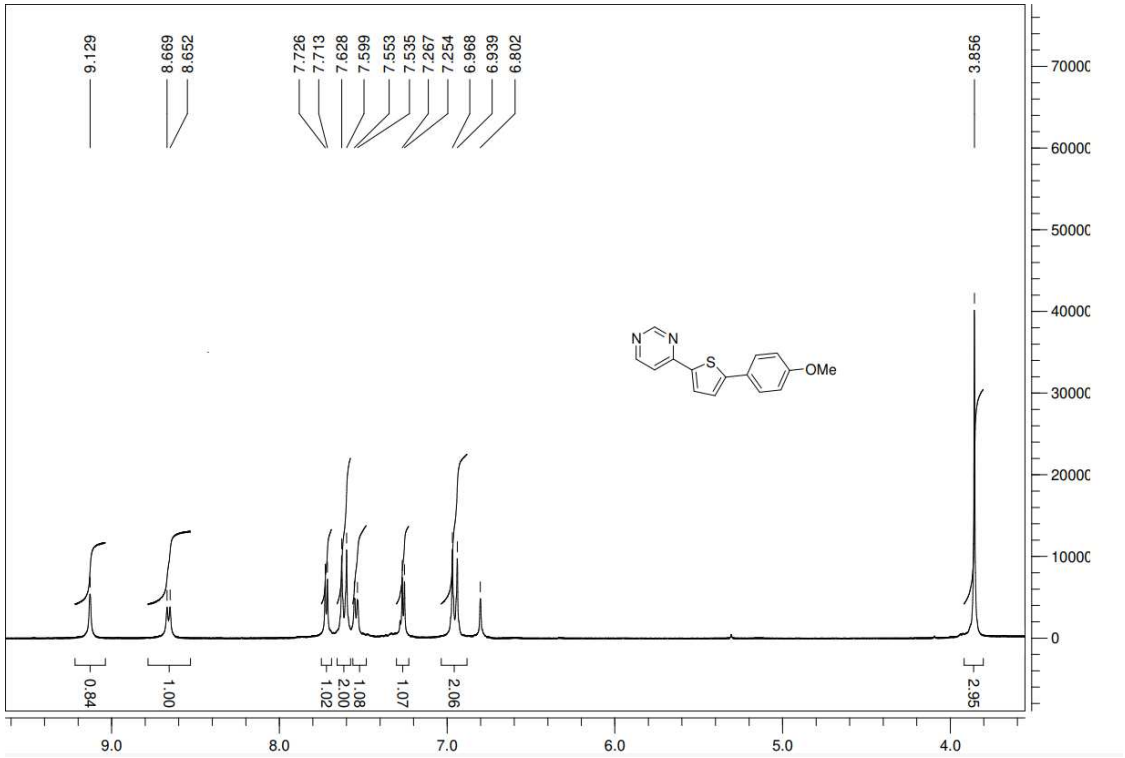

Figure S27. ^{1}H NMR spectrum of compound **3OMe** (300 MHz, $CDCl_3$).

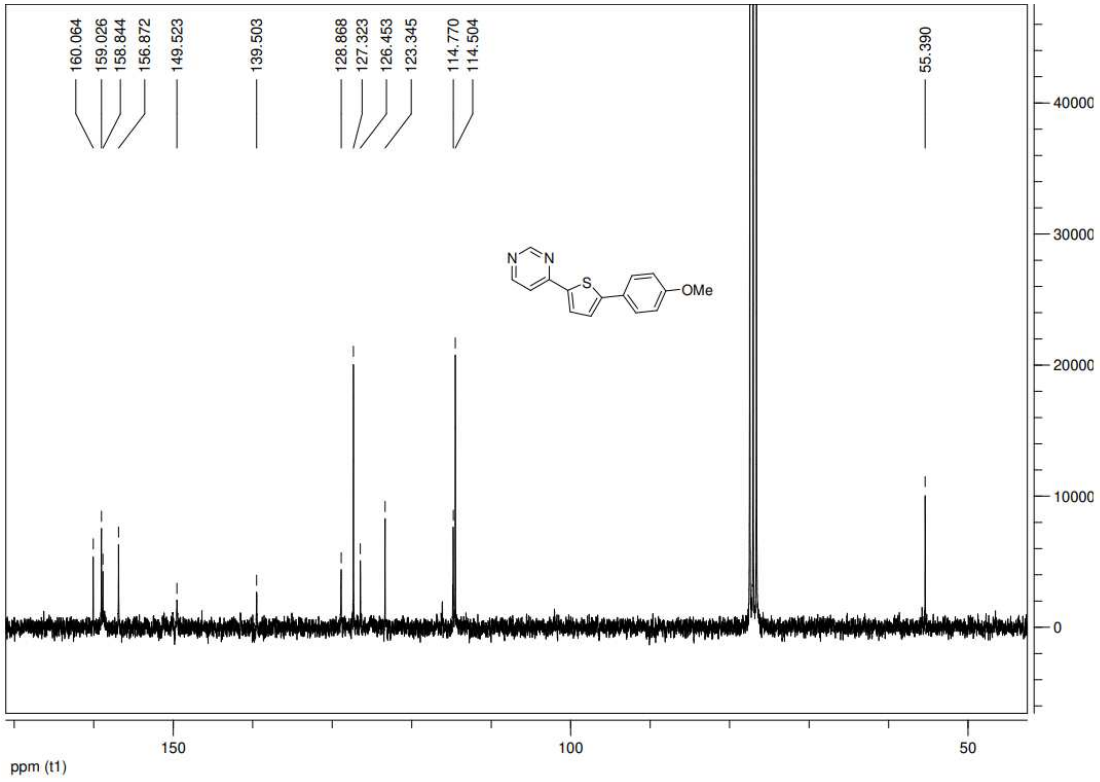

Figure S28. ^{13}C NMR spectrum of compound **3OMe** (75 MHz, $CDCl_3$).